Acta Astronautica 102 (2014) 190–199

Contents lists available at ScienceDirect

Acta Astronautica

journal homepage: www.elsevier.com/locate/actaastro

Tour of Jupiter Galilean moons: Winning solution of GTOC6

Guido Colasurdo [a], Alessandro Zavoli [a], Alessandro Longo [a], Lorenzo Casalino [b,*], Francesco Simeoni [b]

[a] Sapienza University of Rome, Dipartimento di Ingegneria Meccanica e Aerospaziale, Via Eudossiana 18, 00184 Rome, Italy
[b] Politecnico di Torino, Dipartimento di Ingegneria Meccanica e Aerospaziale, Corso Duca degli Abruzzi 24, 10129 Torino, Italy

ARTICLE INFO

Article history:
Received 23 January 2014
Received in revised form
2 May 2014
Accepted 3 June 2014
Available online 11 June 2014

Keywords:
Trajectory optimization
Flyby
Resonant orbits

ABSTRACT

The paper presents the trajectory designed by the Italian joint team Politecnico di Torino & Sapienza Università di Roma (Team5), winner of the 6th edition of the Global Trajectory Optimization Competition (GTOC6). In the short time available in these competitions, Team5 resorted to basic knowledge, simple tools and a powerful indirect optimization procedure. The mission concerns a 4-year tour of the Jupiter Galilean moons. The paper explains the strategy that was preliminarily devised and eventually implemented by looking for a viable trajectory. The first phase is a capture that moves the spacecraft from the arrival hyperbola to a low-energy orbit around Jupiter. Six series of flybys follow; in each one the spacecraft orbits Jupiter in resonance with a single moon; criteria to construct efficient chains of resonant flybys are presented. Transfer legs move the spacecraft from resonance with a moon to another one; precise phasing of the relevant moons is required; mission opportunities in a 11-year launch window are found by assuming ballistic trajectories and coplanar circular orbits for the Jovian satellites. The actual trajectory is found by using an indirect technique.

1. Introduction to the GTOC 6 problem

Global trajectory optimization competition has always intrigued challengers with sophisticated and difficult-to-solve problems. The 6th edition (GTOC6) has not betrayed expectations: indeed the Outer Planet Mission Analysis Group of Jet Propulsion Laboratory, winner of the previous edition, proposed a complex multi-gravity-assist 4-year tour of the main Jupiter satellites (the Galilean moons Io, Europa, Ganymede, and Callisto). The goal was to flyby all these moons, mapping their surfaces, and collecting the highest score. Useful points were scored according to the position of the hyperbola pericenter over the moon surface, which was purposely tailored as a 32-face football. Available points ranged from zero (if the pericenter was over an already-covered face) to three, according to the face position; points were doubled for Europa flybys. Allowed altitude to score points ranged from 50 km to 2000 km, even though higher flybys were permitted. Initial conditions were the spacecraft distance from Jupiter (1000 Jupiter radii, R_J) and the magnitude of the velocity vector with respect to the planet (3.4 km/s). Electric propulsion was available (specific impulse and maximum thrust were 2000s and 0.1 N, respectively); the tour should last less than 4 years in a 11-year launch window. Details can be found in [1].

The problem proposed by JPL is very complex, but a rationale is embedded in it and an adequate mission (i.e., a high-score solution for the competition) can be devised without exploiting any "standard" global optimization technique. An attentive analysis of the underlying physics provides basic guidelines for the mission design; further

* Corresponding author.
E-mail addresses: guido.colasurdo@uniroma1.it (G. Colasurdo), alessandro.zavoli@uniroma1.it (A. Zavoli), alessandro.longo@uniroma1.it (A. Longo), lorenzo.casalino@polito.it (L. Casalino), francesco.simeoni@polito.it (F. Simeoni).

http://dx.doi.org/10.1016/j.actaastro.2014.06.003
0094-5765/

ideas to improve the trajectory emerged during the definition of the mission and were progressively implemented.

The basic idea consists in a fast capture followed by a series of consecutive passages around every Galilean moon by exploiting resonant orbits [2,3]. A rapid evaluation states that time is not sufficient to cover all 128 faces, and that available mass should be almost entirely devoted to the payment of penalties related to low perijoves. In any case, due to the huge mass of Jupiter, electric propulsion provides, in comparison, very low thrust-acceleration, which can be useful only for episodic, but necessary, corrections. A complete coverage of Io and Europa (Eu) is suggested by the very short period of the former and the score bonus when hitting the latter. Callisto (Ca) and Ganimede (Ga) will be hit flying only over the faces that give high score, or are useful to insert the spacecraft into the required resonances.

The envisaged solution consisted of a capture that puts the spacecraft into a Ca-resonant orbit. The spacecraft then moves inward, reducing its energy to enter in resonance with Ga, Eu and Io, in this sequence. Trajectory design is conceptually split in three parts:

- capture (from 1000 R_J to the first Ca-resonant flyby);
- resonant flybys;
- transfer legs between moons.

In this frame, some variants of the strategy were discovered and introduced. Transfers between moons resulted more difficult than envisaged, as a precise phasing of the bodies is required, also because of the low thrust-acceleration. The problem is made more difficult by the orbital resonance between adjacent moons that is typically 2:1; Ca and Ga do not obey this rule, but their resonance 7:3 is even more critical in the frame of the complete mission.

The trajectory scoring $J=311$ has won GTOC6, but at that time was not considered as globally optimal, even though the merit index appeared to be close enough to maximum achievable score. Indeed in the months following the official competition, another team was able to achieve $J=316$, resorting in this case to techniques that are typical of global optimization [4].

2. Capture

This section describes the part of the trajectory which moves the spacecraft from the initial hyperbola to the first of a series of Ca-resonant flybys. The flight along this branch of the trajectory is very difficult: propulsion is used during the capture maneuver to achieve the most suitable magnitude and direction of relative velocity at flybys, as well as to overcome imperfect phasing between the relevant moons. A presentation of the tools used precedes a description of the actual trajectory for capture.

2.1. Tool description

The preliminary design of the capture is crucial to attain the actual trajectory, which is eventually obtained by using an indirect optimization technique. In order to define a proper capture strategy, a revised version of the

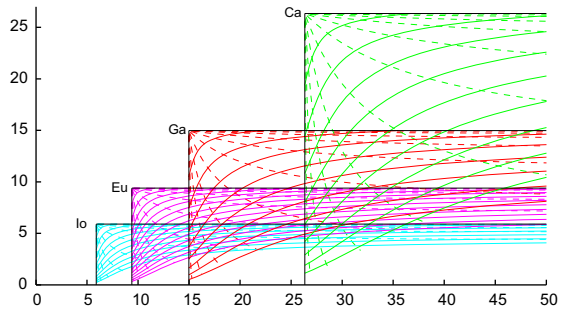

Fig. 1. Tisserand graph for the Galilean moons of Jupiter: $\mathbf{v}_\infty$ contour lines (solid) are drawn at steps of 25% of the moon circular velocity; pump-angle lines (dashed) at steps of 15°.

Tisserand graph [5–8] was adopted, as it permits a better insight into the problem. This kind of graph is useful for preliminary design of ballistic trajectories of a spacecraft that exploits gravity assists in a multibody system; a simplifying hypothesis assumes that secondary bodies move in coplanar circular orbits. The user visualizes, in a simple and fast way, how a gravity-assist changes the orbit of a spacecraft which moves in the fundamental plane of the system. The revised Tisserand graph uses apoapsis and periapsis radii as Cartesian coordinates. The r_a–r_p plot allows a clearer vision of the spacecraft orbit with respect to similar plots (such as Periapsis-Energy [9] or Periapsis-Period [10]); on the other hand, it is not suitable for representing hyperbolic trajectories.

The Tisserand graph for Jupiter and its system of Galilean moons is shown in Fig. 1. For each moon, v_∞ contours (equivalent to lines with a constant value of the Tisserand parameter) are drawn; these solid lines are crossed by dotted curves that indicate the pump angle α, which is the angle between the satellite velocity $\overline{V}_s$ and the hyperbolic excess velocity $\vec{v}_\infty$. Each solid line represents all the possible apoapsis–periapsis pairs attainable with that v_∞ level. In practice, not all of them are reachable from any given initial condition because the maximum $\vec{v}_\infty$−rotation, hence the set of attainable orbits, is constrained by the minimum height allowed during flyby.

In the present problem, a single flyby is not capable of transferring the spacecraft from the initial hyperbola into an elliptic orbit, and a sequence of at least two gravity-assists is needed. After this hard-brake phase, several other flybys are required to reduce the orbital energy to a value compatible with the envisaged moon tour. By choosing the first elliptic orbit already in resonance with a moon, consecutive resonant flybys of that moon could be exploited to attain a fast reduction of the spacecraft orbital energy, without issuing any further phasing constraint. A more complex maneuver is however required for the GTOC6 problem, as described in the following.

An example of Tisserand graph suitable for the design of a flyby chain is shown in Fig. 2. To this end, straight lines, corresponding to spacecraft orbits in resonance $n_s:n_{sc}$ with the satellite,[1] are added. Points representing

[1] The spacecraft, after n_{sc} revolutions around Jupiter, reencounters in the same place the satellite that, in turn, has completed n_s orbits.

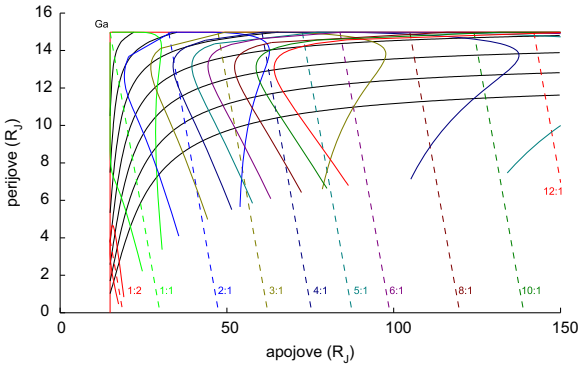

Fig. 2. Example of a Tisserand graph. Resonant orbits and maximum rotation domain for several Ga resonances. Dotted lines denote resonant orbits; each resonance and the related flyby limits share the same color. (For interpretation of the references to color in this figure caption, the reader is referred to the web version of this paper.)

the spacecraft orbits in a chain must lay on the same v_∞-level (ballistic trajectory) and must belong to one of the considered resonances (resonant flybys). Pump angles of consecutive orbits must differ less than the maximum allowed value of $\vec{v}_\infty$−rotation, which depends on the flyby minimum height and the gravitational parameter of the moon. As a visual aid for checking the last requirement, two curves for each resonance were added to the plot, corresponding to the maximum (clockwise or counterclockwise) $\vec{v}_\infty$−rotation that can be obtained by performing a flyby for that level of v_∞. The group of reachable orbits starting from a certain resonance encompasses all the points of the graph between the limit curves. A second set of curves, corresponding to the maximum height for a valid-score flyby, would also be useful; it is omitted for the sake of a simpler figure.

Only v_∞ levels relative to Ga are drawn; constant pump-angle curves were removed for the sake of clearness. An effective flyby requires a $\vec{v}_\infty$−magnitude sufficiently high, but after reaching the maximum effectiveness, the $\vec{v}_\infty$−rotation becomes progressively smaller as the $\vec{v}_\infty$−magnitude increases; therefore, too high values of v_∞ are not desirable to attain fast energy reduction.

2.2. The envisaged capture

The capture phase starts with a Ca flyby, immediately followed by a Ga gravity assist, in order to put the spacecraft into an elliptic orbit. Energy and period reduction are then obtained by a sequence of Ga flybys; as time is the scarcest resource in this problem, Ganimede was chosen to speed up the capture, being sufficiently fast and much heavier than Io and Europe). An initial triple Ca–Ga–Io gravity assist was considered but soon discharged as it would put the spacecraft into a highly elliptic orbit with excessive relative velocity with respect to the external moons, due to the low perijove resulting from Io encounter. Other reasons recommend a solution involving only Ca and Ga. First, in the hard-brake phase the spacecraft approaches Ganimede with large values of v_∞ (5–6 km/s) whereas lower values (2–2.5 km/s) are required for an efficient injection into 1:1 Ca-resonant orbit; the presence of an exterior massive body (Ca) is useful to reduce v_∞. Second, the capture maneuver can be replicated after each Ca–Ga synodic period (that is nearly 12.5 days) and the most favorable window, which allows a good phasing with the interior satellites, can be freely selected later in the competition.

Eventually, a capture beginning with inward Ca-flyby and outward Ga-flyby was selected among several possible variants. These gravity assists could insert the spacecraft either into a 10:1 or an 8:1 Ga-resonant orbit that ferries the spacecraft to a sequence of high-v_∞ Ga-flybys. The latter solution requires a larger use of propulsion, but is interesting because it allows a Ga back-face hit among several front passages. It has been adopted in the winning trajectory, even though, a posteriori, the other solution seems to be capable of a more efficient global strategy, achieving a higher final score. When a 2:1 Ga-resonant orbit has been achieved, a complex Ga–Ca–Ga–Ca trajectory leg begins: a Ga-flyby sends the spacecraft to Ca, whose gravity reduces the eccentricity and allows for a low-v_∞ Ga-flyby, which finally returns the spacecraft to Ca for insertion into a 1:1 resonant orbit.

The time-length of the sequence of high-v_∞ Ga-flybys, exploited to reduce the orbital period, is dictated by the envisaged Ga–Ca–Ga–Ca maneuver, which demands a precise phasing between these two bodies, when the spacecraft leaves Ganimede. Due to the Ca–Ga resonance, the required phasing cannot be obtained (in a reasonable amount of time) only by waiting an integer number of Ga periods (that is, only by exploiting perfect ballistic resonant orbits). Indeed, the proper phasing was obtained by issuing a trajectory that, at one of these flybys, leaves Ga outward and intercepts it inward at a different place along the orbit. This maneuver permits to move backward the Ga intercept point and is effective in changing the Ga-phase with respect to Ca.

In the winning solution, after the hard-brake maneuver, the spacecraft flies a 8:1 Ga-resonant orbit: then it is injected by a flyby into an almost 4:1 orbit, which permits the change of the arrival to Ga from outward to inward. Finally, additional resonant orbits (3.1, 2:1, 3:1, and 2:1) are covered before the Ga–Ca–Ga–Ca transfer begins. The correct phasing for the Ga–Ca–Ga–Ca transfer was achieved in a bit less than 22 Ga periods (measured from the first Ga flyby at the end of the hard-brake phase). The strategy of the capture maneuver is presented and explained by the Tisserand diagram in Fig. 3. Planar views of the trajectory in the Jupiter fundamental plane are shown in Figs. 4 and 5. Throughout this paper, flybys are numbered according to their actual sequence; when necessary a letter indicates the relevant moon.

In principle, the same capture maneuver may be delayed and carried out after each Ca-Ga synodic period. Indeed, the angular positions of Ca–Ga are shifted in space by almost 90° after each synodic period[2]; thus, after four synodic periods the trajectory has the same orientation in space. Results showed that, due to satellite eccentricity and

[2] Ca–Ga are nearly in a 7:3 resonance, which leads to a synodic period of about 3/4 Ca period, hence to a phase shifting of $+\frac{3}{2}\pi$ or $-\frac{1}{2}\pi$.

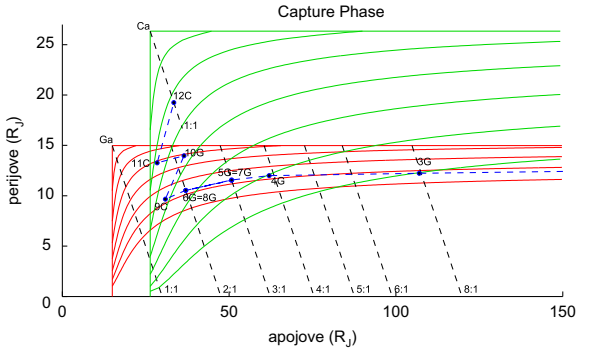

Fig. 3. Capture in the Tisserand graph. Points indicate the orbits just before the corresponding flyby. Notice that flyby 3G moves the spacecraft to an "almost" resonant orbit, thus changing the position of the encounter with Ganymede.

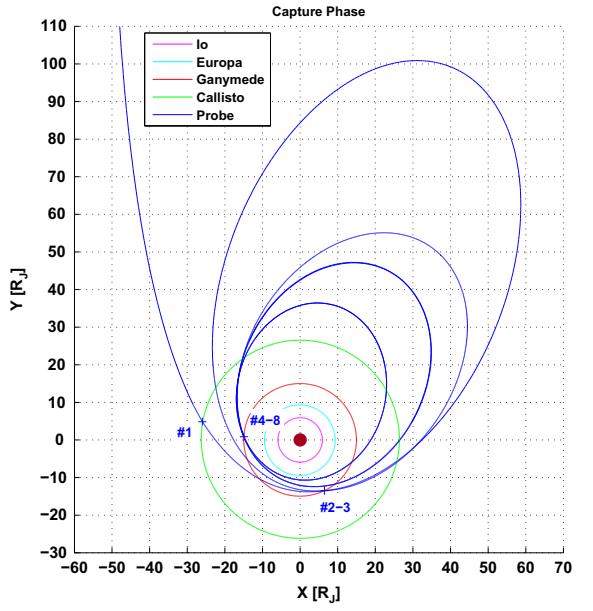

Fig. 4. Winning trajectory. Capture phase. Legs are flown counterclockwise.

inclination, only a mission opportunity out of 4 offers good performance (with the first good opportunity being the third in the 11-year launch window). Only this subset of about 80 opportunities, which occur at intervals of approximately 50 days, has been considered during the competition.

2.3. *Indirect optimization*

The actual 3D maneuver for capture was searched for and defined by using the indirect optimization method [11,12] that Team5 routinely uses [13–16]. The same approach was used for moving the spacecraft from resonance with a moon to another. The capture maneuver (up to GA flyby) and each transfer from one moon to another one, including the Ga–Ca–Ga–Ca gravity assisted transfer, were separately optimized. Constraints on v_∞ magnitude and/or direction were introduced when required by the satellite coverage strategy.

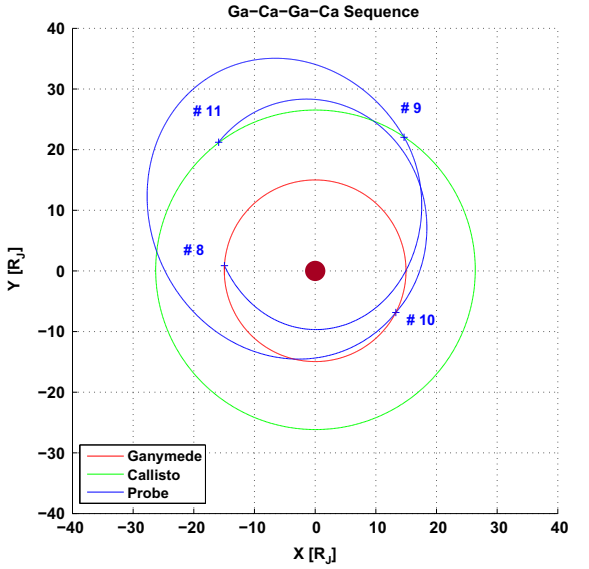

Fig. 5. Winning trajectory. Ga–Ca–Ga–Ca transfer. Legs are flown counterclockwise.

The trajectory is split into arcs, whose time-lengths are additional unknowns of the problem. Arcs join where control (e.g., thrust magnitude) and/or state variables are discontinuous (gravity assists). The theory of optimal control provides the thrust direction and the additional boundary conditions that complete the augmented differential problem (state and adjoint equations). In particular, the switch function is enforced to be zero at boundaries where the engine is switched on or off. Special conditions are necessary for optimality at boundaries where the spacecraft receives gravity assist from a moon. These conditions were first presented for unconstrained flybys [13], and then for constrained height of hyperbola pericenter [14].

The numerical problem is solved by means of a shooting procedure based on Newton's method. The search for a suitable tentative solution is a very difficult task. Some techniques have been proposed in the literature, even though they were not strictly necessary in the present case. Team5 resorts mainly to knowledge of orbital mechanics and spacecraft propulsion for a proper estimation of unknown times and state and adjoint variables.

3. Moon coverage via resonant flybys

A modular strategy has been developed to grant the minimum-time and/or the minimum-penalty coverage of the moons' surfaces. It consists in performing several consecutive flybys of the same satellite, keeping the spacecraft into satellite-resonant orbits. During a chain of flybys, in a pure Keplerian motion, the encounters with the moon always take place after an integer number of moon revolutions and the incoming $\vec{v}_\infty$ to a flyby has the same magnitude and components as the outgoing $\vec{v}_\infty$ from the previous one. Nevertheless, this leaves enough freedom to design a complete coverage: performing resonant orbits at a different inclination and resonance allows the design of

long sequences of flybys, aimed to a complete coverage or, in some case, to a coverage that is purposely kept partial.

Each sequence is inserted between two transfer legs: one coming from the previous satellite and arriving to the current one and the other departing from the current moon, going to the following one. The time-length of the flyby sequence, which determines the time gap between the arrival and departure transfer legs, is a multiple of the satellite period and it is shortened as much as possible, compatibly with the phasing requirements of the following transfer legs. The magnitude of $\vec{v}_\infty$ is maintained during the flyby sequence and must be equal to the $\vec{v}_\infty$−magnitude of both arriving and departing transfer legs. Suitable values for $\vec{v}_\infty$ are provided by the Tisserand graph, looking for transfer legs close to a Hohmann transfer, that is, having apocenter a bit larger than the orbit of the exterior moon and pericenter a bit smaller than the orbit of the internal moon.

3.1. Reference frame

The grid, on which the performance index is built upon, is assigned in a body fixed reference frame $\{\boldsymbol{b}\} = \{\hat{b}_1, \hat{b}_2, \hat{b}_3\}$, defined as

$$\hat{b}_1 = -\frac{\vec{r}_{sat}(t)}{\|\vec{r}_{sat}(t)\|}, \quad \hat{b}_2 = \hat{b}_3 \times \hat{b}_1,$$
$$\hat{b}3 = \vec{r}_{sat}(t) \times \frac{\vec{V}_{sat}(t)}{\|\vec{r}_{sat}(t) \times \vec{V}_{sat}(t)\|} \tag{1}$$

A suitable reference frame $\{\boldsymbol{k}\} = \{\hat{k}_1, \hat{k}_2, \hat{k}_3\}$, fixed to the moon inertial velocity $\vec{v}_{sat}$, is introduced:

$$\hat{k}_1 = \hat{k}_2 \times \hat{k}_3, \quad \hat{k}_2 = \vec{r}_{sat}(t) \times \frac{\vec{V}_{sat}(t)}{\|\vec{r}_{sat}(t) \times \vec{V}_{sat}(t)\|}, \quad \hat{k}_3 = \frac{\vec{V}_{sat}(t)}{\|\vec{V}_{sat}(t)\|} \tag{2}$$

as it has been found useful to define the coverage strategy. The relationship between the body reference frame $\{\boldsymbol{b}\}$ and the velocity fixed frame $\{\boldsymbol{k}\}$ is shown in Fig. 6. The relative rotation between the two systems is connected to the satellite flight path angle γ. Hence the configuration of the two frames is a function of the flyby position on the satellite orbit.

The spacecraft orbit around Jupiter depends on the direction of $\vec{v}_\infty$ in the $\{\boldsymbol{k}\}$ frame, which can be expressed using two angles, namely L_a (latitude) and L_o (longitude) with reference to the equatorial plane in the $\{\boldsymbol{k}\}$ frame, defined by unit vectors $\hat{k}_1$ and $\hat{k}_2$. This plane is perpendicular to the body equatorial plane in the $\{\boldsymbol{b}\}$ frame. Pump and crank angles in the literature [6] correspond to colatitude and longitude in this frame, respectively. When $\vec{v}_\infty$−magnitude and resonance ratio are assigned, so is the pump angle and, consequently, the latitude. The loci of $\vec{v}_\infty$-direction correspond to parallels on a spherical grid based on the $\{\boldsymbol{k}\}$ frame.

Jupiter satellites move in almost coplanar orbits very close to the base (i.e., fundamental) plane of the reference frame centered on Jupiter. Longitudes 0° and $\pm 180^\circ$ for $\vec{v}_\infty$ imply spacecraft orbits in the planetocentric base plane (zero-inclination); the maximum inclination is attained for $L_o = \pm 90^\circ$. With respect to the moon orbital plane, flybys occur at the descending node of the spacecraft orbit for $-180^\circ < L_o < 0^\circ$ (ascending node for $0^\circ < L_o < 180^\circ$); the spacecraft motion is inbound for $-90^\circ < L_o < 90^\circ$; otherwise it is outbound.

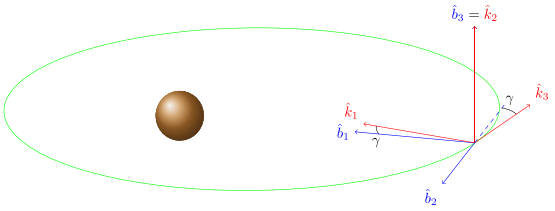

Fig. 6. Moon-centered reference frames.

Moons' orbits are almost circular, angle γ is very low and, in a preliminary analysis, the boundaries of the 32 target faces could be drawn in the $\{\boldsymbol{k}\}$ frame without significant loss of precision. Therefore, only the $\{\boldsymbol{k}\}$ frame is used in the search for the flyby strategy. In Fig. 7 the Callisto face map is presented in the $\{\boldsymbol{k}\}$ frame. When the entire range of γ, that is, all the possible positions of the encounter are considered, the border of the faces becomes a thick band that accounts for the possible rotation between the two frames. In order to avoid tricky circumstances, which would imply the loss of some score points, the pericenter position is held at some distance from the thick band during all the preliminary design process.

The flyby sequence was studied on this grid by analyzing the pericenter position related to a flyby that moves the spacecraft from a resonant orbit to another. If the previous resonance ratio is maintained (crank maneuver), the resulting pericenter will be located on the equator, while the outgoing velocity will be at the same latitude as the incoming one. If the resonance ratio is changed, the $\vec{v}_\infty$ latitude changes and this implies that a nonzero latitude of pericenter is obtained.

During a complete flyby sequence, the fastest 1:1 resonance is usually exploited and the pericenter travels along the equator. At the right time, the pericenter position is moved at different latitudes by changing the resonance, moving onto a n_s:n_{sc} orbit ($n_s \neq n_{sc}$), and then back to the 1:1 resonant orbit to hit the body opposite face. The immediate return is mandatory in order to contain time-length of the whole sequence. The first and last flybys do not obey this rule. Instead, they are used to rotate $\vec{v}_\infty$ from the direction (i.e., the latitude) assigned by the incoming transfer leg to the basic 1:1 resonance and from this, after the flyby sequence has been completed, to the direction required by the outgoing transfer leg. In some cases, these adjustments can be done directly in a single step; a passage through an intermediate resonant orbit is necessary in other cases.

Fig. 7 shows, as an example, a flyby over Ca surface: coming from a 1:1 resonant orbit (incoming $\vec{v}_\infty$ is here depicted by a magenta cross) the spacecraft moves either to a 3:2 or to a 1:1 resonant orbit. The outgoing $\vec{v}_\infty$ (blue dot) is constrained on the blue parallels, whose latitude is related to the new resonance ratio: the upper parallel

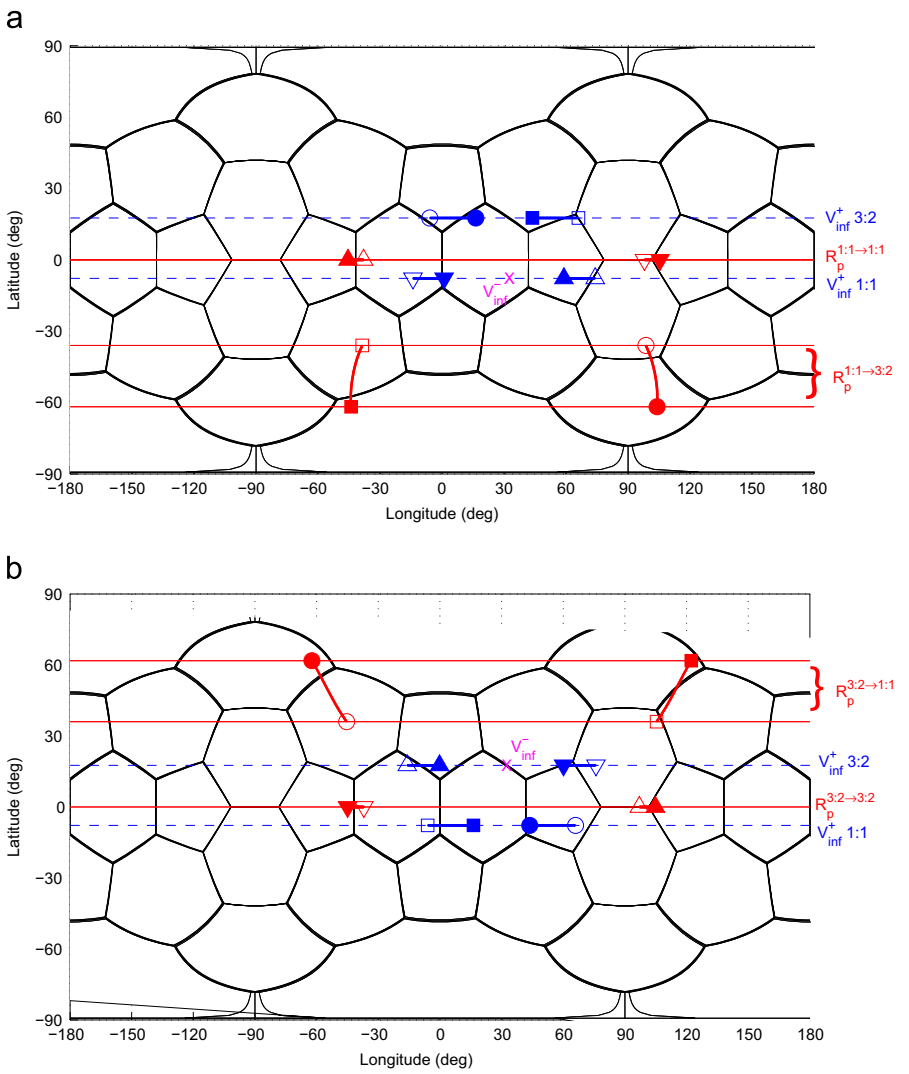

Fig. 7. Visual representation in the $\{\boldsymbol{k}\}$ frame of a few exemplifying flyby maneuvers (Callisto, $\mathbf{v}_\infty = 2.22$ km/s). (a) Incoming resonance=1:1. (b) Incoming resonance=3:2. (For interpretation of the references to color in this figure caption, the reader is referred to the web version of this paper.)

corresponds to a 3:2 resonant orbit, the lower to a 1:1. Flyby height, instead, defines $\vec{v}_\infty$ longitudes: the lower the height, the farther away the longitudes of outgoing and incoming $\vec{v}_\infty$. There is another degree of freedom in the longitude, since the $\vec{v}_\infty$−rotation may be clockwise (on the left side of incoming $\vec{v}_\infty$) or counterclockwise (on the right). As far as locations of pericenter are concerned, flyby height has a relevant role on both coordinates. Pericenter loci are presented as red bands in Fig. 7; the lower bands apply when passing to 3:2 resonance. When the 1:1 resonance is maintained pericenters are on the red equatorial line. The pericenters related to the minimum/maximum flyby height are marked with the same symbol as the corresponding $\vec{v}_\infty$. Fig. 7(b) refers to a spacecraft arriving on a 3:2 resonant orbit. If this resonance is kept, the pericenter position moves along the equatorial line: this pericenter movement is more efficiently obtained by flying two consecutive 1:1 resonant orbits. Passage from 3:2 to 1:1 resonance permits the coverage of the northern hemisphere. In the example presented in Fig. 7, the passage from 1:1 to 3:2 resonant orbit permits the coverage of the southernmost 10 faces, whereas returning to 1:1 resonance provides the northernmost 10 faces; 12 equatorial faces can be hit by maintaining 1:1resonance. Usually the complete coverage of the moon surface is obtained by a continuous leftward (or rightward) movement of the hyperbola pericenter until a complete revolution is performed. Pericenter direction

$$\hat{r}_p = \vec{r}_p/|\vec{r}_p| = (\vec{v}_{\infty-} - \vec{v}_{\infty+})/|\vec{v}_{\infty-} - \vec{v}_{\infty+}| \tag{3}$$

is presented in Fig. 8 for a maneuver that moves the spacecraft from resonance 3:2 to resonance 1:1.

4. Transfer legs

Transfer legs aim to move the spacecraft from a resonant orbit with a moon to a resonant orbit with a different moon. Formally, each transfer leg starts with the

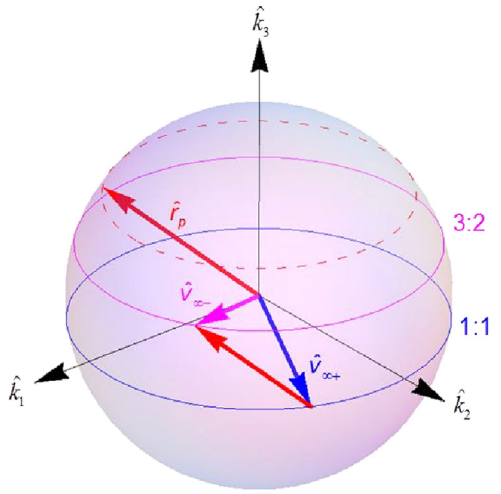

Fig. 8. Pericenter direction moving from 3:2 to 1:1 Ca-resonant orbit.

spacecraft leaving a moon with hyperbolic excess velocity of assigned magnitude and free direction; the leg ends when the spacecraft reaches the target moon, before the gravitational assist that will put it into a resonant orbit. As the available thrust is very small in comparison to gravitational force, the transfer is essentially ballistic; hence, a correct phasing of the relevant moons is mandatory.

After the capture phase and the sequence of Ca flybys, the first transfer leg moves the spacecraft from Ca to Ga. Only few degrees of freedom are left to the user. The Ca–Ga phasing at departure depends only on the time-length of the Ca coverage maneuver (i.e., the number of Callisto revolutions elapsed during its coverage); almost no variation is produced by shifting the mission departure date by an integer number of Ca–Ga synodic periods, as the relative phase between the two moons would be almost the same. Indeed, the phasing repeats almost exactly if the Ca coverage is lengthened by three revolutions, as Ca and Ga are almost in resonance 3:7.

The magnitude of the hyperbolic excess velocity at Ca departure is fixed, being the same as at the end of the Ga–Ca–Ga–Ca leg which completed the capture phase (coverage maneuvers are ballistic). The transfer is also constrained by the requirement of sufficiently low v_∞ at Ga arrival, necessary to perform an efficient Ga coverage. Eventually, the only freedom is the choice of $\vec{v}_\infty$-direction and additional length of Ca coverage (0, 1, or 2 Ca revolutions).

More freedom is left for designing the remaining part of the mission which, in the early days of the competition, encompassed a Ga–Eu–Io transfer and was replaced, in the later days, by a more complex Ga–Eu–Io–Eu–Ga sequence, which proved to be more performing. The date of departure from Ga is dictated by the previous legs of the trajectory, but is still not fixed: after a preliminary trajectory for the capture and the Ca–Ga transfer has been devised, actual opportunities repeat after multiples of four Ca–Ga synodic periods.

A preliminary search for favorable transfer opportunities (i.e., epochs presenting a proper phasing between Jovian satellites) has been addressed by a parametric analysis under few simplifying assumptions. Moon orbits are assumed to be circular and coplanar, transfer legs and resonant flybys to be completely ballistic. As a result, moon coverage lasts always an integer number of satellite revolutions; $\vec{v}_\infty$−magnitude at arrival to and departure from a satellite is the same, but $\vec{v}_\infty$−rotation is at a certain extent free. The study of the transfer legs becomes independent of the moons' coverage.

In the coplanar case, the geometric parameters of the transfer ellipse are completely defined once the magnitudes of departing and arrival $\vec{v}_\infty$ are set. Each transfer orbit provides four different opportunities for moving the spacecraft from a moon to the following one within a complete revolution, resulting from the four intersections of the ellipse with the two circular orbits. These transfer types are named I–O (i.e., Inbound–Outbound), I–I, O–I, and O–O according to the radial component of the velocity at departure and arrival [9]. For each opportunity, when the initial positions of both satellites are known, one can evaluate the transfer flight-time and check if the spacecraft intercepts the target moon. In practice, for given $\vec{v}_\infty$−magnitude and moons' phasing at departure, an iterative procedure – based on a secant algorithm – was set up in order to find the arrival $\vec{v}_\infty$−magnitude, which ensures the respect of the phasing constraint. The search is restricted to a small range of v_∞ that, for each Jovian satellite, allow the desired moon coverage within a minimum number of revolution.[3] A sequence of legs (i.e., a tour) is obtained by joining more legs together. Once the solution of a leg is found, the following one is studied by assuming as departure date the sum of the arrival epoch and of the coverage time, and as $\vec{v}_\infty$−magnitude at departure the same value as at arrival on that moon.

In order to increase the number of transfer opportunities, multiple revolutions on the transfer ellipse were also considered, despite being time-consuming. Further opportunities were created by considering moons' coverages up to two periods longer than the minimum necessary time[4]; instead, maneuvers which could reduce the coverage time-length (such as back-flips or inbound/outbound changes) were not investigated due to the short time available for the competition, and also to the probable growth of phasing problems. In order to find out candidate tours, a parametric analysis was performed by varying

- $\vec{v}_\infty$−magnitude departing from Ga (within a range of permissible values)
- initial date (i.e., date of arrival to Ga after Callisto coverage)

[3] Team5 used the following ranges of values: 2.30–2.40 km/s for Io, 1.90–2.10 km/s for Eu, 2.40–2.60 km/s for Ga, and 2.10–2.30 km/s for Ca.

[4] Any computed sequence can be easily lengthened by an integer number of periods, while preserving the resonant strategy, in two ways: by changing a resonance, e.g., from 4:5 to 5:4, or by inserting a further 1:1 resonant orbit. The former solution has been used during the first sequence of Eu-resonant flybys, achieving the correct phasing while maintaining the number of flybys. The latter was instead used on Io, involving the repetition of a face to improve the phasing with Eu.

Table 1
Summary of resonant flybys sequences in the final solution.

Moon	No. of flybys	No. of hit faces	Satellite Revs	Resonances used	Notes
Ca	20	20	25	1:1 2:3 3:2	2 Faces during capture
Ga	26	24	37	1:1 3:2	6 Faces during capture
Eu	28	28	52	1:1 4:5 5:4 4:3	No repetitions
Io	33	32	71	1:1 5:4 4:3	Outbound arrival, inbound departure 1 face repeated
Eu (II)	4	4	9	1:1 4:5 4:3	Eu coverage completed
Ga (II)	2	2	1	1:1	1 Face missing

Table 2
Summary of all flybys exploited during the mission.

Moon	No. of flybys	No. of hit faces	No. of repetitions
Callisto	22	22	0
Ganymede	36	31	5
Europa	32	32	0
Io	33	32	1
Total	123	117	6

plus, for each leg

- coverage time on the departing moon (expressed in terms of number of moon revolutions during the coverage);
- transfer type (I–I, I–O, O–I, or O–O);
- number of spacecraft revolutions on the transfer ellipse (between 0 and 3).

A similar procedure has been used to analyze the simpler transfer leg from Ca to Ga.

Team5 found that actual opportunities for moving between satellites were scarce; in particular between the innermost moons. A great part of the opportunities found by using the previous approach was discharged when the real maneuver, involving the "true" moon orbits, was searched for by means of an indirect technique. Actually, in most cases, phasing and transfer time-length were found to be correct, whereas the largest errors were related to $\vec{v}_\infty$−magnitude at arrival (which unfortunately has to fall into a specific range of values for a proper moon coverage).

5. Winning trajectory

This section describes the trajectory designed by Team5, and its evolution from the first idea to the final winning version. In the initial design, the capture maneuver involved several flybys of both Ga and Ca, all aimed to reduce the spacecraft velocity: the hyperbola pericenters were in the northern hemisphere of $\{\boldsymbol{k}\}$ frame. The last Ga-flyby addressed the probe to Ca, where the spacecraft started the first out of four series of resonant flybys during its descent from Ca to Io, via Ga and Eu (corresponding score $J=308$).

In this first attempt, during the capture maneuver, the spacecraft entered a 10:1 Ga-resonant orbit after the first encounter of this moon. All the following Ga-flybys were

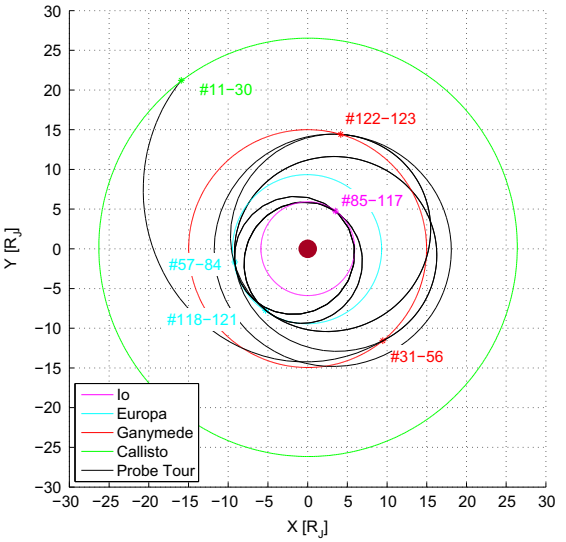

Fig. 9. Winning trajectory. Tour phase. Flyby locations are marked with asterisks.

over faces of the northern hemisphere, often already hit; four southern faces, instead, were not covered during the mission. The capture maneuver cannot be faster because of phasing requirements, but the initial use of an 8:1 Ga-resonance, instead of the 10:1 previously adopted, leaves two additional Ga-periods available to permit the passage of the spacecraft, after 2:1 resonance is achieved, back to 3:1; this passage requires a flyby over a southern face, adding one point and rising the score to $J=309$.

A single sequence of resonant flybys was initially envisaged for Europa. The complete coverage of its surface, that is compulsory for high score, required four more passages on the northern hemisphere, dictated by the inward motion of the spacecraft from Ga to Io. The only possibility to avoid duplicate hits is splitting the Eu-resonant flybys; a second series of resonant flybys occurs when flying outward after Io surface has been entirely covered. The modified strategy saves flight-time, which is used to reach again Ga hitting two of his southern faces. These two additional points raised the final score to $J=311$.

Tables 1 and 2 summarize flyby data for the winning trajectory. Figs. 4, 5, 9 and 10 provide a visual representation; noticeable features are described in the following:

- *Callisto*: Ten low-score faces (totaling 12 points) have been neglected, due the long period of Ca orbit; 2:3

and 1:1 resonances, having short duration without significant mass penalties, were preferred; 3:2 resonance is occasionally exploited to reach the highest latitude faces.

- *Ganymede*: High latitude faces were hit during capture or at the end of mission. The 3:2 and 1:1 resonant orbits are preferred in order to save time (2:3 resonance cannot be attained from 1:1 resonant orbits).
- *Europa*: Two flyby sequences based on 4:5, 5:4, 4:3 and 1:1 resonances. Resonance ratio near to 1 is required by Europa low mass. Global coverage is obtained without any face repetition.

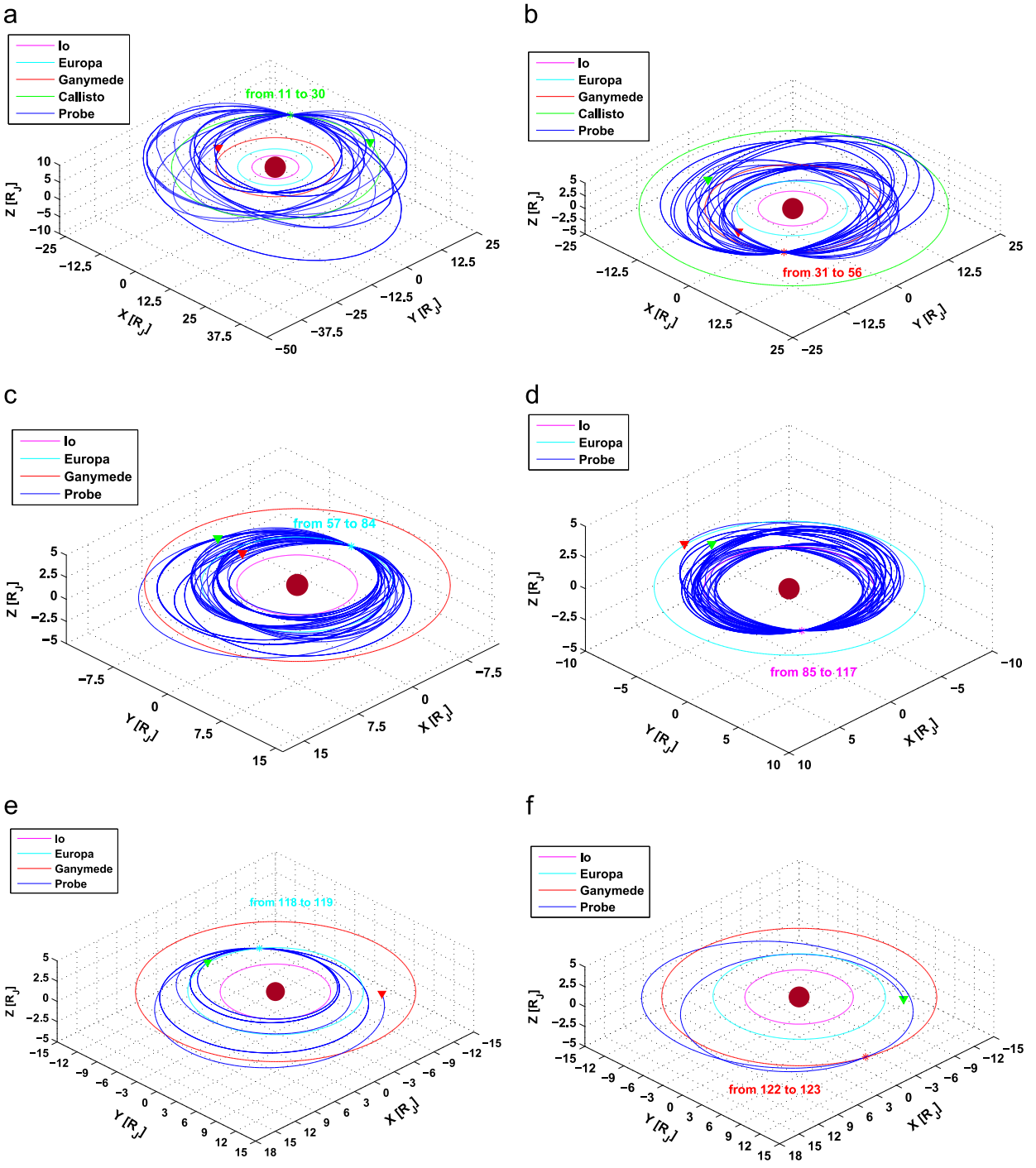

Fig. 10. Winning trajectory. Resonant orbits flown during the moon coverages. Flyby location is marked with an asterisk; green and red triangles highlight the initial and the final points of the coverage phase. (a) Callisto Tour. (b) 1st Ganimede Tour. (c) 1st Europa Tour. (c) Io Tour. (d) 2nd Europa Tour. (e) 2nd Ganimede Tour. (For interpretation of the references to color in this figure caption, the reader is referred to the web version of this paper.)

- *Io*: A single sequence of flybys with just one face taken twice to fulfill phasing requirements; the only case with transition from outbound arrival to inbound departure. 5:4, 4:3 and 1:1 resonant orbits were chosen to contain mass penalties.

During the competition, Team5 had no time to study a further possible improvement. The winning trajectory presents duplicate hits of several Ga faces. The capture using 10:1 Ga-resonance for the first elliptic orbit in the mission would permit a more regular coverage of Ga during both the capture and the following resonant flyby sequence. The initial hyperbolic leg approaching Jupiter would be faster (additional time could be saved using a thrust-coast-brake control) and the Ga-flyby sequence would be two Ga-periods shorter. The saved time would permit the completion of Ga coverage, returning from Eu at the end of mission; a final Ca-hit might be the icing on the cake.

6. Conclusions

In GTOC6, the most recent edition of the Global Trajectory Optimization Competition, Team5 proposed a solution that, on principle, was based on the complete coverage of each satellite, moving from the outer to the inner Galilean moon. This kind of coverage can be analyzed and fully defined independently of the epoch and of the relative phasing between satellites. The capture, that is the passage from the initial hyperbola to a low-energy ellipse, and the transfer of resonance between moons were analyzed using a classical indirect method after selecting a viable mission opportunity by considering ballistic trajectories and moons moving on circular coplanar orbits.

This approach to the problem, completed by marginal upgrades, permitted the achievement of a very high score, without the need of huge computational resources. Further improvements require the reduction of the average time between flybys, which is achieved by frequent movements between the moons. Resonant orbits with high n_s can be canceled by exploiting favorable phasing of the relevant moons. This result requires a modern approach, typical of global optimization. This kind of technique has been brilliantly developed and adopted by ESA-ACT & Hong Kong University (Team6), who got the second position in the final ranking.

Acknowledgments

The authors would like to thank Prof. Dario Pastrone, Francesca Letizia, and Stefano Federici who were also members of Team5 and contributed to the victory.

References

[1] A.E. Petropoulos, Problem Description for the 6th Global Trajectory Optimisation Competition. URL: ⟨http://www.esa.int/gsp/ACT/doc/MAD/ACT-RPT-MAD-GTOC6-problem_stmt.pdf⟩, 10 September 2012.
[2] A. Wolf, Touring the saturnian system, Space Sci. Rev. 104 (1–4) (2002) 101–128, http://dx.doi.org/10.1023/A:1023692724823.
[3] B. Buffington, S. Campagnola, A. Petropoulos, Europa multiple-flyby trajectory design, in: Guidance, Navigation, and Control and Co-located Conferences, American Institute of Aeronautics and Astronautics, 2012. http://dx.doi.org/10.2514/6.2012-5069.
[4] D. Izzo, L.F. Simões, M. Märtens, G.C. de Croon, A. Heritier, C.H. Yam, Search for a grand tour of the jupiter galilean moons, in: Proceeding of the 15th Annual Conference on Genetic and Evolutionary Computation Conference, ACM, New York, NY, USA, 2013, pp. 1301–1308. http://dx.doi.org/10.1145/2463372.2463524.
[5] J. Miller, C. Weeks, Application of Tisserand's criterion to the design of gravity assist trajectories, in: Guidance, Navigation, and Control and Co-located Conferences, American Institute of Aeronautics and Astronautics, 2002. http://dx.doi.org/10.2514/6.2002-4717.
[6] N.J. Strange, R. Russell, B. Buffington, Mapping the V-infinity Globe, in: AIAA/AAS Space Flight Mechanics Meeting, AAS Paper 07-277, 2007.
[7] K.W. Kloster, A.E. Petropoulos, J.M. Longuski, Europa orbiter tour design with Io gravity assists, Acta Astronaut. 68 (7–8) (2011) 931–946, http://dx.doi.org/10.1016/j.actaastro.2010.08.041. URL: ⟨http://www.sciencedirect.com/science/article/pii/S0094576510003395⟩.
[8] S. Campagnola, A. Boutonnet, J. Schoenmaekers, D.J. Grebow, A.E. Petropoulos, R.P. Russell, Tisserand-leveraging transfers, in: AAS/AIAA Space Flight Mechanics Meeting, Charleston, SC, American Astronautical Society Paper, 2012, pp. 12–185.
[9] N.J. Strange, J.M. Longuski, Graphical method for gravity-assist trajectory design, J. Spacecr. Rockets 39 (1) (2002) 9–16.
[10] A.F. Heaton, N.J. Strange, J.M. Longuski, E.P. Bonfiglio, Automated design of the Europa orbiter tour, J. Spacecr. Rockets 39 (1) (2002) 17–22.
[11] D. Lawden, Optimal trajectories for space navigation, Butterworths Mathematical Texts, Butterworths, 1963 URL: ⟨http://books.google.it/books?id=jLFxAAAAMAAJ⟩.
[12] A.E. Bryson, Y.C. Ho, Applied Optimal Control, Hemisphere Publishing, New York, 1975.
[13] L. Casalino, G. Colasurdo, D. Pastrone, Optimization procedure for preliminary design of opposition-class mars missions, J. Guid. Control Dyn. 21 (1) (1998) 134–140.
[14] L. Casalino, G. Colasurdo, D. Pastrone, Optimal low-thrust escape trajectories using gravity assist, J. Guid. Control Dyn. 22 (5) (1999) 637–642, http://dx.doi.org/10.2514/2.4451.
[15] G. Colasurdo, L. Casalino, Optimal control law for interplanetary trajectories with nonideal solar sail, J. Spacecr. Rockets 40 (2) (2003) 260–265, http://dx.doi.org/10.2514/2.3941.
[16] M. La Mantia, L. Casalino, Indirect optimization of low-thrust capture trajectories, J. Guid. Control Dyn. 29 (4) (2006) 1011–1014, http://dx.doi.org/10.2514/1.18986.